

REPORT DOCUMENTATION PAGE				Form Approved OMB No. 0704-0188	
<p>The public reporting burden for this collection of information is estimated to average 1 hour per response, including the time for reviewing instructions, searching existing data sources, gathering and maintaining the data needed, and completing and reviewing the collection of information. Send comments regarding this burden estimate or any other aspect of this collection of information, including suggestions for reducing the burden, to the Department of Defense, Executive Services and Communications Directorate (0704-0188). Respondents should be aware that notwithstanding any other provision of law, no person shall be subject to any penalty for failing to comply with a collection of information if it does not display a currently valid OMB control number.</p> <p>PLEASE DO NOT RETURN YOUR FORM TO THE ABOVE ORGANIZATION.</p>					
1. REPORT DATE (DD-MM-YYYY)	2. REPORT TYPE		3. DATES COVERED (From - To)		
	FINAL REPORT		01 Oct 2004 - 30 Sep 2006		
4. TITLE AND SUBTITLE			5a. CONTRACT NUMBER		
SOFTWARE DEVELOPMENT FOR MODELING HIGH POWER SOLID STATE SLAB LASERS			5b. GRANT NUMBER FA9550-05-1-0005		
			5c. PROGRAM ELEMENT NUMBER 61102F		
6. AUTHOR(S) DR BASS			5d. PROJECT NUMBER 2305/GX		
			5e. TASK NUMBER		
			5f. WORK UNIT NUMBER		
7. PERFORMING ORGANIZATION NAME(S) AND ADDRESS(ES) UNIVERSITY OF CENTRAL FLORIDA 4000 CENTRAL FLORIDA BLVD ORLANDO FL 32816-8005				8. PERFORMING ORGANIZATION REPORT NUMBER	
9. SPONSORING/MONITORING AGENCY NAME(S) AND ADDRESS(ES) AF OFFICE OF SCIENTIFIC RESEARCH 875 NORTH RANDOLPH STREET ROOM 3112 ARLINGTON VA 22203 DR HAROLD WEINSTOCK				10. SPONSOR/MONITOR'S ACRONYM(S)	
				11. SPONSOR/MONITOR'S REPORT NUMBER(S)	
12. DISTRIBUTION/AVAILABILITY STATEMENT DISTRIBUTION STATEMENT A: UNLIMITED AFRL-SR-AR-TR-07-0104					
13. SUPPLEMENTARY NOTES					
14. ABSTRACT We will extend this study to smaller grain sizes to determine if the trend observed continues or if the curve eventually turns down. During this period we identified an error in our earlier work on depolarization in crystalline lasers. This error, was caused by a problem in writing the reduced form of the 4th rank tensor that gives the piezo optic effect. It was essential to have found this error as we started evaluating depolarization losses in ceramic crystal lasers. These lasers are of general interest and are in use in the Textron Thin-Zag laser. We discuss the error, its correction and the evaluation of depolarization losses in ceramic crystals in this report. Since this report was first drafted we detected an error in our method of calculating the path of a ray through a random array of crystallites. This has been corrected and the results are being revised.					
15. SUBJECT TERMS					
16. SECURITY CLASSIFICATION OF:		17. LIMITATION OF ABSTRACT	18. NUMBER OF PAGES	19a. NAME OF RESPONSIBLE PERSON	
a. REPORT	b. ABSTRACT			c. THIS PAGE	19b. TELEPHONE NUMBER (Include area code)

Final Report for

Air Force Office of Scientific Research
AFOSR Contract No. FA9550051005

Entitled

Software Development for Modeling High Power Solid State Slab Lasers

UCF Account No. 65016128

By

Michael Bass, Principal Investigator
College of Optics and Photonics/CREOL
University of Central Florida
Orlando, FL 32816
Tel: (407) 823-6977
E-mail: bass@creol.ucf.edu

February, 2007

20070406432

I. Description of Activities

During this period we identified an error in our earlier work on depolarization in crystalline lasers. This error, was caused by a problem in writing the reduced form of the 4th rank tensor that gives the piezo optic effect. It was essential to have found this error as we started evaluating depolarization losses in ceramic crystal lasers. These lasers are of general interest and are in use in the Textron Thin-Zag laser. We discuss the error, its correction and the evaluation of depolarization losses in ceramic crystals in this report.

I. Depolarization Losses

Calculations of the depolarization loss in single crystal have been performed with a correction to the method of our previous work [1]. This method has been extended to calculate the depolarization loss in a ceramic crystal slab. It has been found that there is a dependence of the overall depolarization loss of the ceramic crystal on the grain size. To understand how to model birefringence and depolarization loss in ceramic crystal lasers one needs to review the models which have been developed to analyze the problem in single crystal lasers. Our group has previously performed calculations of depolarization losses in single crystal Yb:YAG and Nd:YAG lasers [1,2].

A material that is birefringent is defined as one in which there is a difference between two principal indices of refraction. The dielectric impermeability tensor of a material relates the optical field to the response of a material to that field. It must be used to find the change in the indices of refraction of a crystalline material that is stressed as is a laser gain medium. Because it is a second rank tensor, the dielectric impermeability can be used in tensor mathematics involving physical properties of the crystal. The index of refraction which is not a tensor quantity should not be treated as one. Stress is the physical quantity that gives rise to a change in the dielectric impermeability and thus the principal indices of refraction. The relationship between stress and the dielectric impermeability is:

$$\Delta B_{ij} = \pi_{ijkl} \sigma_{kl}, \quad (1)$$

where ΔB_{ij} is the change in the second-rank dielectric impermeability tensor, π_{ijkl} is the fourth-rank piezo-optic tensor, and σ_{kl} is the second-rank stress tensor. Each of the indices range from 1 to 3. Since the values of the piezo-optic tensor are given in the crystal coordinate system and the values for stress are in the laboratory coordinate system, a transformation must be performed so that the two quantities are in the same basis before multiplying them. To simplify the calculations a reduced suffix notation is often employed that is described in *Physical Properties of Crystals* [3]. Using reduction methods in Ref. 3, the number of suffixes can be reduced such that Equation (1) becomes

$$\Delta B_m = \pi_{mn} \sigma_n \quad (2)$$

where each of the indices now range from 1 to 6.

When performing the transformation, the reduced piezo-optic tensor should be expanded into its full-suffix form, transformed, and then reduced again. It is important to follow Nye's convention closely when applying the reduced suffix notation. One source was found to have left out several factors of $1/2$ in the piezo-optic tensor which are necessary in order to bring the notation into agreement with Nye's notation [4]. Chen et. al. mention this problem as well as the problem of another paper treating the index of refraction as a tensor quantity [1] which is only applicable in a limiting circumstance. An expression equivalent to Eq. 2, for the dielectric impermeability is

$$\Delta B_m = p_{mn} \epsilon_n, \quad (3)$$

where p is the elasto-optic tensor and ϵ is the symmetric strain tensor. It is presented here in the reduced-suffix form. Results obtained by either calculation should be equivalent. Therefore after calculating the dielectric impermeability using Eq. (2), the calculation can be compared with the result of Eq. (3).

Another issue arising in Ref. 1 is of the values given therein for the compliance tensor. Since Dixon measured the values of the elasto-optic coefficients in 1966 [5], it is possible to calculate the piezo-optic coefficients using the relationship

$$\pi_{mn} = p_{mr} s_m \quad (4)$$

where s is the compliance tensor in reduced-suffix form [3]. The values for the compliance tensor are found in A. A. Kaminskii's *Laser Crystals* [6]. Also, the values for the stiffness tensor can be found there. The stiffness tensor can be experimentally determined and the compliance tensor can be calculated from the stiffness tensor. Stiffness and compliance are inversely related such that the matrices c and s satisfy

$$c \cdot s = I \quad (5)$$

where I is identity matrix. Given that one knows the stiffness tensor, the compliance can be calculated by taking the inverse of the stiffness tensor. Using the values for the stiffness tensor given in Ref. 5, one will find that the stiffness tensor is not invertible unless one assumes symmetry in the strain tensor which is what has been assumed in Ref. 3. There the strain is explicitly represented as the symmetric part of the deformation. Under this assumption one can invert the stiffness tensor, but a modified version of the identity matrix must be used. The fourth-rank identity tensor with assumed symmetry for the strain tensor can be found in Walpole's paper "Fourth-Rank Tensors of the Thirty-Two Crystal Classes: Multiplication Tables" [6]. It is given as:

$$I_{ijkl} = \frac{1}{2}(\delta_{ik}\delta_{jl} + \delta_{il}\delta_{jk}) \quad (6)$$

The general stiffness tensor is not invertible under the identity $I_{ijkl} = \delta_{ik}\delta_{jl}$ but is invertible under the identity given in Eq. (6). In Ref. 1 the stiffness tensor from *Laser Crystals* was incorrectly inverted and a factor of four appeared in the values for the s_{44} component of the compliance tensor. The correct values for the compliance tensor, found in Ref. 4, are

$$s_{11} = 3.59 \cdot 10^{-12} \text{ Pa}^{-1},$$

$$s_{12} = -0.90 \cdot 10^{-12} \text{ Pa}^{-1}, \text{ and} \quad (7)$$

$$s_{44} = 8.69 \cdot 10^{-12} \text{ Pa}^{-1}.$$

With the correct values of the compliance tensor one can solve for the piezo-optic tensor using Eq. (4). After transforming from the crystal coordinate system into the laboratory coordinate system, the values for the piezo-optic tensor are found to be:

$$\begin{aligned} \pi_{11} &= -3.0217 \cdot 10^{-13} & \pi_{12} &= 1.1114 \cdot 10^{-13} \\ \pi_{13} &= 1.717 \cdot 10^{-13} & \pi_{14} &= -1.7129 \cdot 10^{-13} \cdot \cos(3\Phi) \\ \pi_{15} &= -1.7129 \cdot 10^{-13} \cdot \sin(3\Phi) & \pi_{33} &= -3.6273 \cdot 10^{-13} \\ \pi_{44} &= -2.9219 \cdot 10^{-13} & \pi_{66} &= -4.1331 \cdot 10^{-13} \end{aligned} \quad (8)$$

where Φ is the cut angle. Using π the calculation in Equation (2) can be performed. This results in the dielectric impermeability tensor for the crystal in the laboratory coordinate system. At this point, a submatrix is extracted from the dielectric impermeability tensor representing the components that will be perpendicular to the direction of propagation. This submatrix is

$$\begin{pmatrix} B_{11} & B_{12} \\ B_{12} & B_{22} \end{pmatrix}, \quad (9)$$

where B_{12} is equivalent to B_{21} , and therefore both are represented by B_{12} . Again, this is in the laboratory coordinate system, but in order to calculate the birefringence the dielectric impermeability must be diagonalized. We therefore find the eigenvalues of the submatrix (9):

$$B_{\pm} = \frac{1}{2}[B_{11} + B_{22} \pm ((B_{11} - B_{22})^2 + 4B_{12}^2)^{\frac{1}{2}}] \quad (10)$$

The eigenvalues are the diagonal elements of the matrix when the matrix is diagonalized. A polarized beam oriented along one of the axes in the diagonalized system would not experience depolarization because for instance:

$$\begin{pmatrix} B_+ & 0 \\ 0 & B_- \end{pmatrix} \begin{pmatrix} 0 \\ 1 \end{pmatrix} = \begin{pmatrix} 0 \\ B_- \end{pmatrix} \quad (11)$$

The index of refraction is related to the dielectric impermeability according to:

$$B_{\pm} = \frac{1}{n_{\pm}^2} \quad (12)$$

Finding the eigenvalues of the dielectric impermeability and then representing it as a diagonalized matrix is equivalent to transforming the dielectric impermeability from the original basis to the basis in which it is diagonalized. Consequently there is an angle of rotation associated with the transformation. We call this angle θ , and from the transformation relationship:

$$B_{ij} = a_{ik} a_{jl} B_{kl} \quad (13)$$

we find

$$\tan(2\theta) = \frac{2B_{12}}{B_{11} - B_{22}}. \quad (14)$$

Also, in Ref. 1 the depolarization loss is given by

$$Loss = \sin^2(2\theta) \sin^2\left(\frac{\delta}{2}\right), \quad (15)$$

where

$$\delta = \frac{2\pi}{\lambda} L(n_+ - n_-) \quad (16)$$

is the phase delay. L is the length of the sample in the direction of propagation and λ is the wavelength.

We applied the corrected values of the compliance tensor to the calculation of depolarization losses in a single crystal Yb:YAG slab through which the rays propagate in a zig-zag fashion (see Fig. (1)). The slab has Brewster ends angled at 30.6 degrees and

is pumped with 9.8 kW of diode power. The calculated losses using our revised model are shown in Fig. (2).

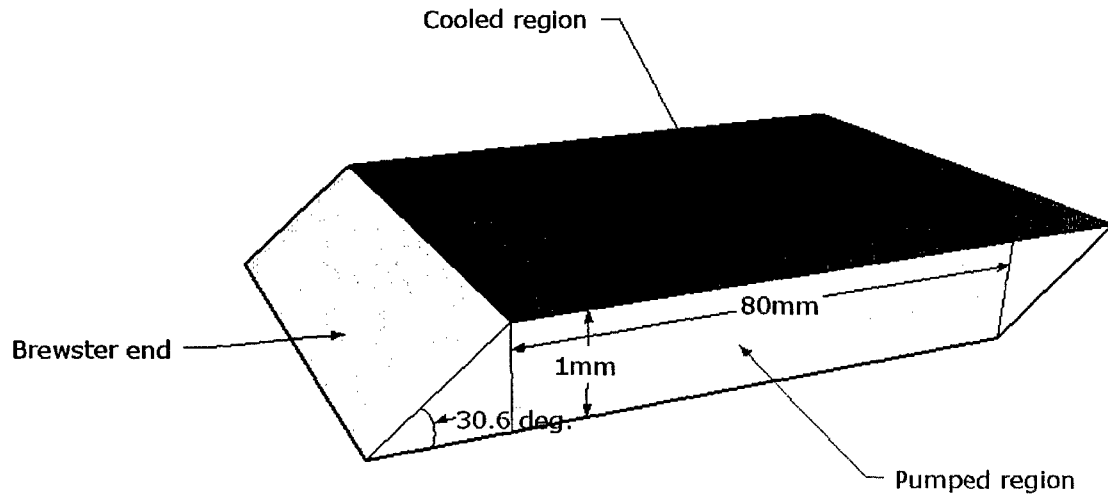


Figure 1: Geometry of the slab used in the simulations of depolarization loss.

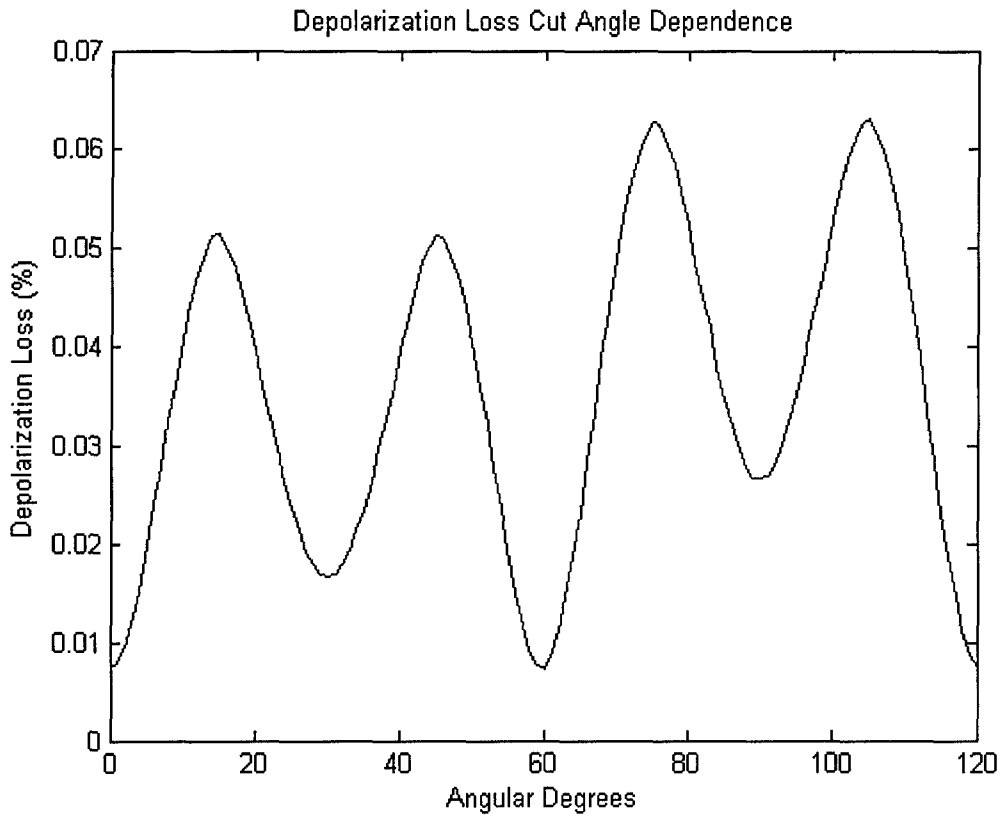


Figure 2: Depolarization loss vs cut angle ϕ in the single Yb:YAG crystal sketched in Fig. 1. The shape of the curve in Fig. (2) is very similar to that found in Ref. 2 but the magnitude of the depolarization loss in Fig. (2) is about an order of magnitude smaller than the values in Ref. 2.

Modeling of the depolarization loss in ceramic crystal was also performed. Because the ceramic crystal is made up of multiple particles oriented randomly, no graph such as that

in Fig. (2) for ceramics can be produced. Instead the effect of the grain size on the depolarization was investigated.

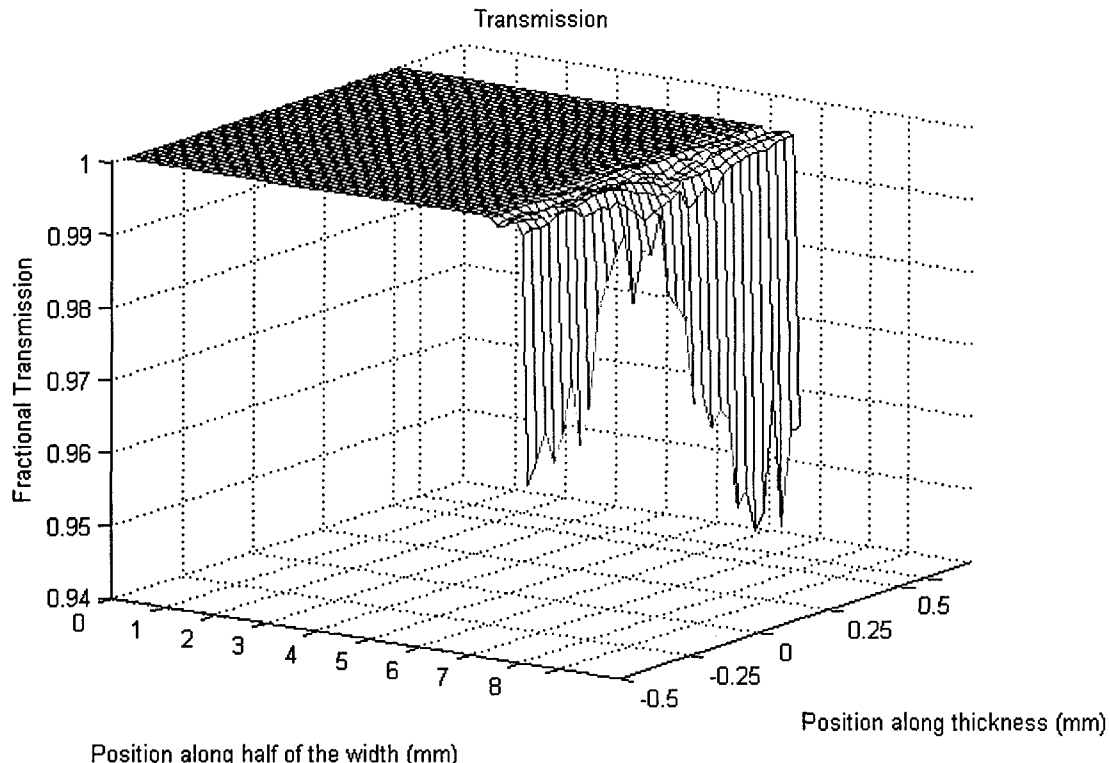


Figure 3: Calculated fractional transmission for the single crystal slab shown in Fig. 1 and pumped as indicated in the text with a cut angle of 75 degrees as a function of the position of the beam as it enters the slab in Fig. 1. The deviations from a transmission of 1.0 are due to depolarization losses. This figure is included here for comparison to the transmission calculated when the same size and shape ceramic crystal slab is similarly pumped as shown in Figure (4).

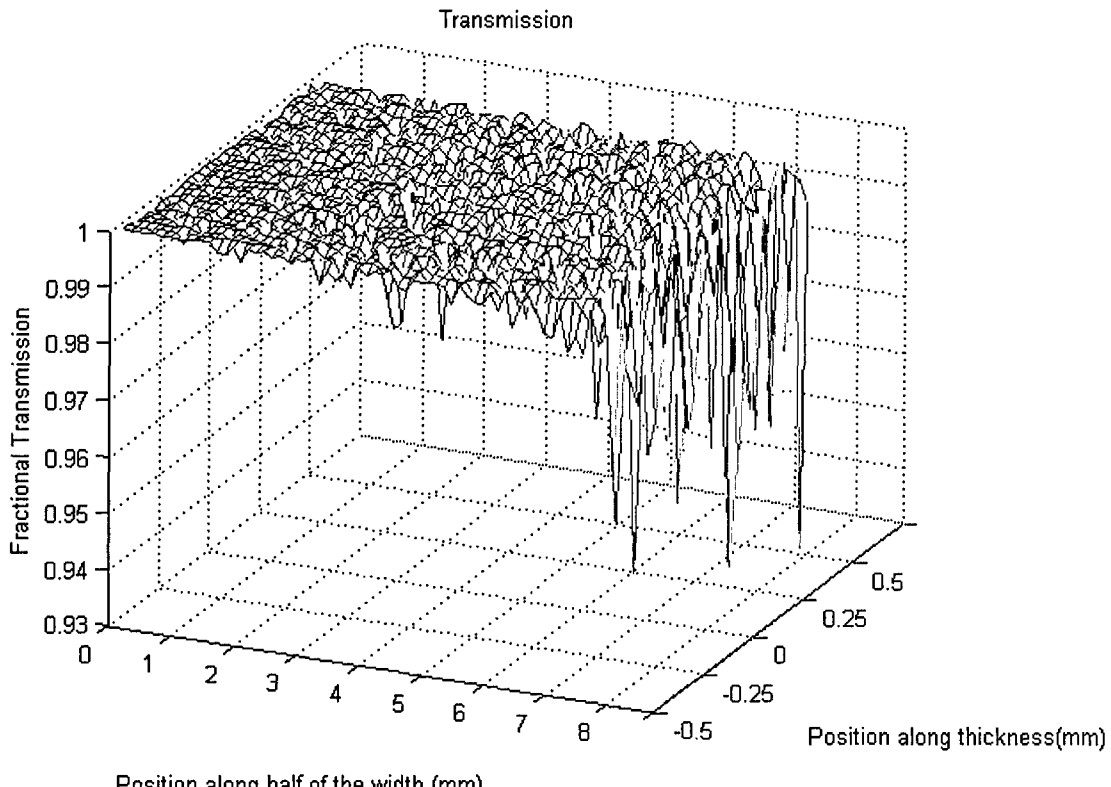


Figure 4: Calculated transmission for a ceramic crystal slab of the same size and shape as shown in Fig. 1 and pumped as indicated in the text as a function of the position of the beam as it enters the slab in Fig. 1. The deviations from a transmission of 1.0 are due to depolarization losses. In this case the grain sizes are assumed to have a normal distribution centered at 20 μm with a standard deviation of 5 μm .

Comparing Figs. 3 and 4 reveals what appears to be noise in the transmission changes due to depolarization loss for the ceramic crystalline laser slab in the mid region of the slab. This is not noise but the result of varying losses due to the randomly oriented crystalline grains that the beam passes through when zig-zagging through the ceramic crystal slab. These losses contribute to the overall depolarization loss resulting in a larger loss than for a similar sized, shaped and stressed single crystal slab.

The dependence of the depolarization loss on grain size was studied and is shown in Fig. (5). The normal distributions of the grain sizes assumed are shown in Fig. (6).

Depolarization Loss Vs. Grain size

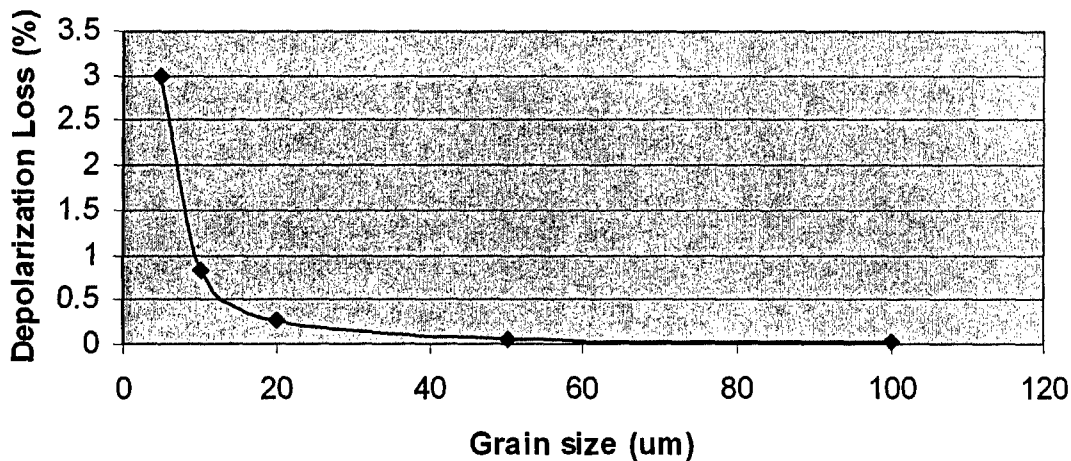


Figure 5: Depolarization loss in ceramic crystal as a function of the grain size.

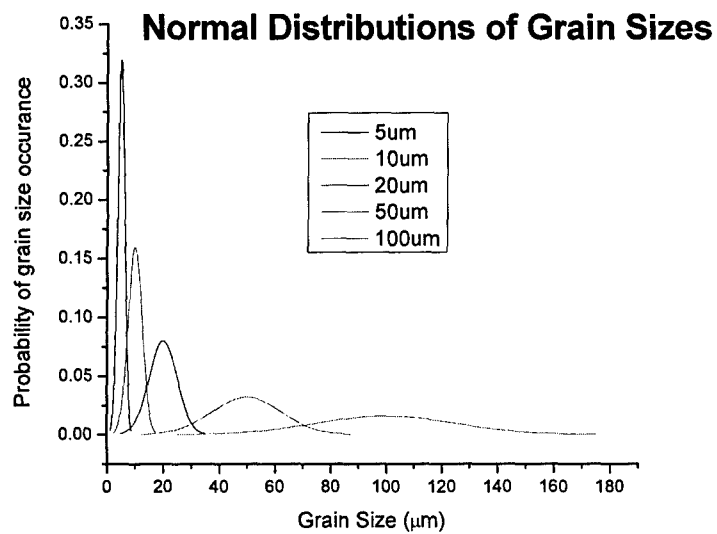


Figure 6: Each of the curves represents a distribution of the grain size for the results in Figure (5)

Figs. 5 and 6 might suggest that the depolarization loss depends on the width of the grain size distribution. To see if this was indeed a significant factor, another distribution was included and the depolarization losses were calculated again for the distribution centered at 100 μm . The added distribution assumed is shown in Fig. 7, and in Fig. 8 we show that no significant difference in depolarization loss could be detected.

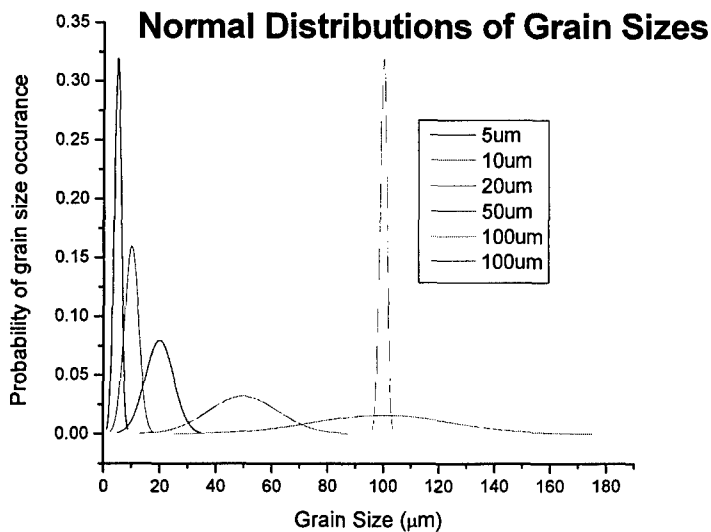


Figure 7: A distribution of grain sizes centered at 100um but with a standard deviation of 1.25 um was included in the data set.

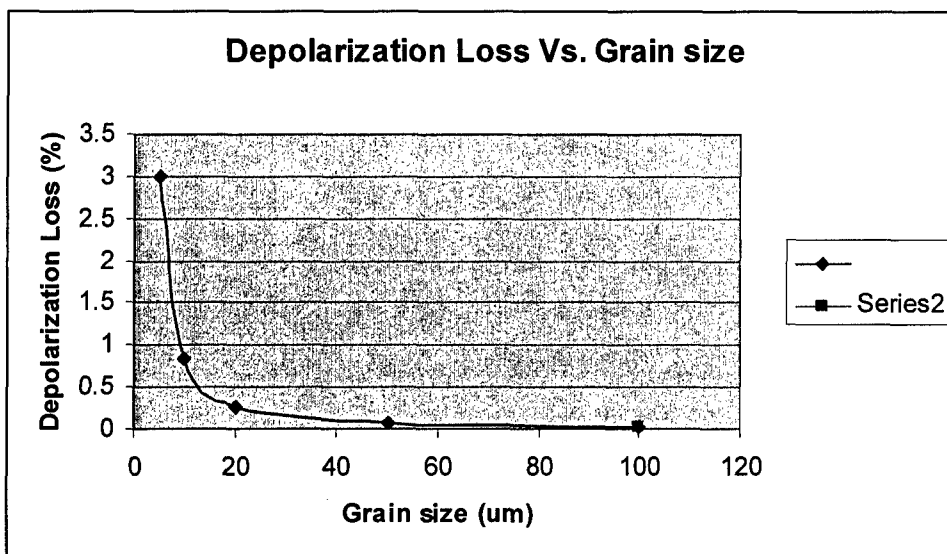


Figure 8: Included here in orange is the data point representing the narrower distribution of grain size at 100um.

From these results, the factor of four correction in our calculations has changed the magnitude of the predicted depolarization loss in the single crystal but not its general shape. Also, there is a notable dependence of the depolarization loss on the grain size. Our results suggest that reducing the grain size below 20 μm risks larger depolarization losses in ceramic crystalline laser media than may be desirable.

We will extend this study to smaller grain sizes to determine if the trend observed continues or if the curve eventually turns down.

Note: Since this report was first drafted we detected an error in our method of calculating the path of a ray through a random array of crystallites. This has been corrected and the results in Figs. 5-8 are being revised.

References

1. “*Calculation of Thermal-Gradient-Induced Stress Birefringence in Slab Lasers—I,*” Ying Chen, Bin Chen, Manoj Kumar R. Patel, and Michael Bass, IEEE Journal of Quantum Electronics **40**, 909-916 (2004)
2. “*Calculation of Thermal-Gradient-Induced Stress Birefringence in Slab Lasers—II,*” Ying Chen, Bin Chen, Manoj K. R. Patel, Aravinda Kar, and Michael Bass, IEEE Journal of Quantum Electronics **40**, 917-928 (2004)
3. *Physical Properties of Crystals: Their Representation by Tensors and Matrices*, J. F. Nye, Oxford University Press, New York (1985).
4. “*Photoelastic effects in Nd :YAG rod and slab lasers,*” Q. Lü, U. Wittrock, S. Dong, Optics and Laser Technology **27**, 95-101 (1995)
5. “*A New Technique for Measuring Magnitudes of Photoelastic Tensors and its Application to Lithium Niobate,*” R. W. Dixon and M. G. Cohen, Applied Physics Letters **8**, 205-207 (1966).
6. *Laser Crystals: Their Physics and Properties*, Alexander A. Kaminskii, Springer (1981).